18th International Conference
ENGINEERING MECHANICS 2012
Svratka, Czech Republic, May 14 – 17, 2012

pp. 543–549
Paper #206

LARGE-SCALE MICRO-FINITE ELEMENT SIMULATION OF COMPRESSIVE BEHAVIOR OF TRABECULAR BONE MICROSTRUCTURE

O. Jiroušek, P. Zlámal *

Abstract: *Microstructural finite element analysis has become a standard technique for evaluation of mechanical properties of trabecular bone. Due to the high complexity of the trabecular bone microstructure, the FE models have a very large number of elements (about 1 million elements per cubic cm in 50 μm^3 resolution). To perform FE analysis of the microstructural FE models based on micro-CT scanning of whole bone samples (e.g. vertebral bodies) it is needed to solve 10^7 – 10^8 equations. This article deals with comparison of approaches using voxel-based microstructural FE models to calculate the overall mechanical properties of trabecular bone.*

Keywords: ***voxel FE models, elastic properties, trabecular bone, parallel computing, MPI***

1. Introduction

Inverse estimation of material properties (namely stiffness and strength) of trabecular bone using FE models of its microstructure is important not only as a nondestructive tool for early prediction of osteoporotic fracture, but can be successfully applied in other research areas, e.g. in animal models to study effect of various growth factors on bone formation.These microstructural FE models are used to perform a numerical simulation of mechanical experiment. Usually, the micro-FE model is subjected to unit load in three mutually perpendicular directions and elastic constants are determined from the 'virtual experiment'.

With the growth of computer power of today's computers it is now possible to solve large systems of algebraic equations arising from discretization of differential equations using the finite element method. This enables to use very detailed FE models of trabecular bone microstructure for inverse determination of their overall mechanical properties [van Rietbergen et al (1999), Niebur et al (2000)]. In these microstructural models, tissue material properties are usually assumed to be isotropic and homogeneous and are determined using either nanoindentation [Rho et al (1997), Zysset et al (1999), Jirousek et al (2011)] or from micromechanical tests performed on individual trabeculae [Jungmann et al (2011), Doktor et al (2011), Lorenzetti et al (2011)].

The early models of the trabecular bone microstructure involved only small volume of the bone [Muller et al (1995)], but solving large number of equations on parallel architectures using either shared [Natarajan (1991)] or distributed memory [Johan el al (1994), Hodgson and Jimack (1997)] architecture enabled to use this inverse modeling to compute the overall stiffness and strength of whole bones [MacNeil et al (2008), Eswaran et al (2007)]. One possibility for FE modeling of whole bones is to use continuum FE models of whole bones [Taddei et al (2004)] with spatially variable material properties, i.e. material properties are prescribed to each finite element based on the tissue density obtained based on the tissue density in the material point [Pahr and Zysset (2009)]. In this case, the inner microstructure is not taken into account and is reflected only by the different density. These FE models are computationally far less demanding, but their ability to reflect the real microstructure as well as changes of the tissue material properties due to metabolic diseases, e.g. deficiency of the bone mineral is at least questionable.

With the advancement of X-ray imaging systems, particularly with growing resolution and physical dimensions of modern X-ray flat panel detectors it is now possible to acquire tomographic images of

*Doc. Ing. Ondřej Jiroušek, Ph.D., Ing. Petr Zlámal: Institute of Theoretical and Applied Mechanics, Prosecká 76, 190 00 Prague 9; CZ, e-mail: {jirousek, zlamal}@itam.cas.cz

whole bones with resolution sufficient to capture its inner structure. These flat panel detectors convert X-ray photons not absorbed by the inspected object into visible-light photons using a scintillating material. A layer of photodiodes converts these photons into electrons which activate corresponding pixels in a layer of amorphous silicone. The activated pixels are used to generate the high-quality, high-resolution digital image in a computer. Modern X-ray flat panel detectors have several megapixel resolution with typical pixel size 50-200 μm.

One possibility to develop the FE model of trabecular bone architecture is to use smooth-boundary tetrahedral models. This technique has been popular in early 1990s but requires extra user intervention to develop these models. Marching Cubes Algorithm [Lorensen and Cline (1987)] is needed to find the surface of the trabecular bone and because of the complexity of the architecture this procedure usually involves user-intervention both in the process of tissue segmentation and in the smoothing/optimization of the surface (triangular) mesh. Moreover, resulting FE models can have even more degrees of freedom than directly generated voxel models.

Easier approach in terms of model development is to convert the segmented 3-D image data to a voxel model. In this procedure, every voxel (spatial pixel) in the sequence of microtomographic images is directly converted to one hexahedral element. It has been shown [Chevalier et al (2007)] that these models can be used for inverse estimation of elastic properties and strength of trabecular bone. Since the procedure to develop a voxel model is quite straightforward it can be used to develop a micro-FE model of whole bones. However, to solve even only a linear static analysis (single solution of a set of linear algebraic equations) large memory is needed to store the sparse system matrix. For example – the volume of an average human vertebral (L4) body is 45×10^3 mm^3. With micro-CT images taken at 50 μm^3 resolution and with average porosity 85%, one gets a FE model with approximately 48 million elements.

In the present study a parallel solution strategy is described for solving such a large problem in parallel utilizing existing open-source programs. Our main aim was to demonstrate the scalability of proconditioned conjugate gradient (PCG) parallel solver for large linear elasticity problems. Two architectures are used, one distributed shared memory (DSM) system (SGI Altix), second shared memory system (Intel Xeon X5560) tested using two problems of different size. The larger problem (rat vertebra) is solved on SGI Altix 4700 series equipped with 56 2-core Intel Itanium-2 processors and SGI's NUMAlink processor interconnect with 288 GB RAM. The smaller problem (sample of human trabecular bone) is solved using a 16-core system based on Intel Xeon X5560 processors with 48 GB RAM. Voxel FE model of rat vertebra is developed based on micro-CT images taken in 50 μm^3 resolution. Total number of unknowns in these models was approximately 14.10^6 and $1{,}7.10^6$, respectively. The models are used for inverse estimation of the rat vertebrae stiffness in the inferosuperior direction and in case of the human bone sample for orthotropic properties inverse calculation.

2. Materials and Methods

2.1. Micro-CT scanning of trabecular bone microstructure

To develop high-resolution micro-FE model of trabecular bone at different resolution, two experiments were performed. In the first experiment, only a cylindrical sample has been extracted from human proximal femur. The sample (diameter 5 mm and height 8 mm) was mounted on a rotating table and placed in a shielded X-ray box. A complete tomography (360 projections, 1° increment) of the sample was performed to capture its microstructure. For the tomographic measurements an X-ray source (Hamamatsu L8601-01 with 5 μm focal spot size) and Medipix-2* (256×256 square pixels, 55×55 μm^2 each) detector were used. Acquired tomographic projections were beam hardening (BH) corrected using a set of aluminum calibrators covering the full attenuation range of the bone specimen using a procedure described in Vavrik and Jakubek (2009).

The second experiment involved scanning whole vertebra. In this case L4 vertebra of a laboratory rat has been chosen. To improve the spatial resolution in this case of a specimen with larger physi-

*Medipix collaboration home page: http://medipix.web.cern.ch/MEDIPIX/

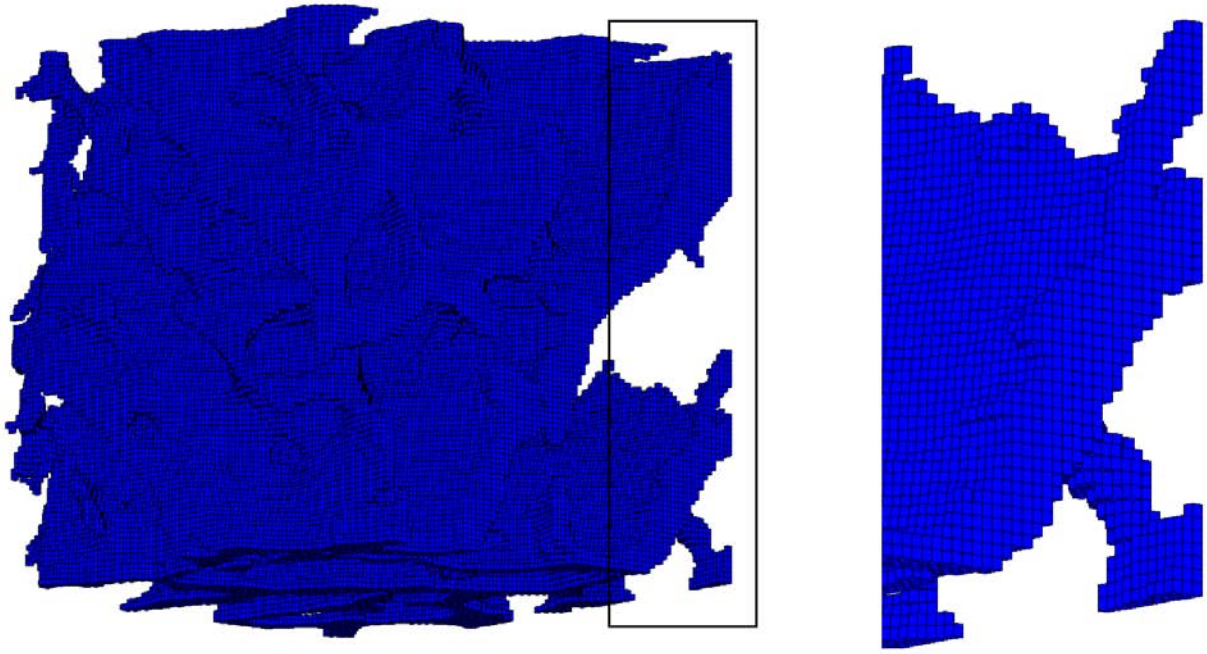

Fig. 1: FE model of the trabecular bone microstructure (left) developed based on the micro-CT image data (100x100x100 voxels) showing the microstructure represented using linear hexahedral elements. Detail (right) showing individual elements.

cal dimensions, a flat panel X-ray detector C7942CA-22 (Hamamatsu Photonics K.K.) with resolution 2368×2240 px and physical dimensions 120×120 mm was used. Scanning sequence consisted of 360 scans with 0.5° step.

2.2. Development of the voxel micro-FE models

The cross-sectional image data were reconstructed from the sinograms using either FBP (filtered back-projection) or OSEM (ordered subsets expectation maximization) methods. Both FBP and OSEM provided similar results with OSEM resulting in more homogeneous background. However, both techniques resulted in a set of images suitable for easy application of segmentation with a global threshold. The threshold value is set automatically based on the Otsu's method with chooses the threshold to minimize the intraclass variance of the black and white pixels [Otsu (1979)].

For the micro-FE model of the vertebra, only a subregion was selected – the cortical shell and internal trabecular structure of the vertebral body was considered. The endplates and the posterior processes has been mathematically removed. These parts were excluded from the inverse computation of the overall stiffness due to simplify the load application and specification of the boundary conditions. Direct conversion from micro-CT volumetric data to voxel micro-FE models requires only setting appropriate threshold to distinguish between the bone and empty space. The threshold value was chosen iteratively using one selected reconstructed cross-section of the vertebra.

2.3. Inverse calculation of the stiffness and strength

To compute the overall stiffness of the vertebral body in the infero-superior direction a unit displacement has been prescribed on the top surface of the vertebral body. The lower surface of the body was fixed (all nodes with minimal z-coordinate were prescribed zero displacements in three directions). Based on our previous nanoindentation results [Jirousek et al (2011)] the tissue-level material properties were prescribed: Young's modulus of elasticity E_{TISSUE}=15 GPa, Poisson's ratio: μ_{TISSUE}=0.2.

From the volume data, 100×100×100 voxels were selected in the middle part for easy comparison of orthotropic elastic properties. The coordinate axes were aligned such as to keep Z-axis in the direction of

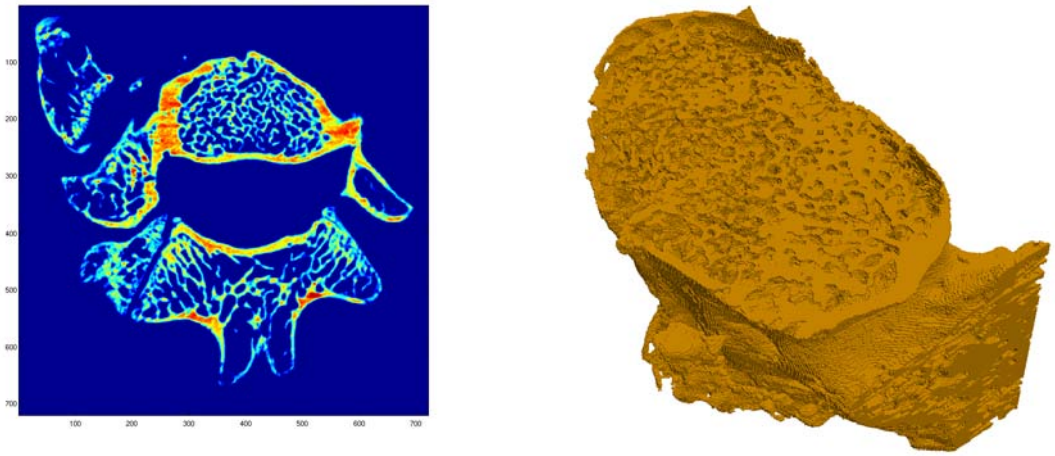

Fig. 2: Cross-sectional image data of the whole rat vertebra and the FE model created from the vertebral body part showing the microstructure represented using hexahedral elements

loading during the experiment. Total number of nodes was 566,790 for the $100\times100\times100$ voxel model and 4,791,142 for the FE model of rat vertebra. Prior the computations, the FE models were verified for mesh connectivity.

2.4. Parallel computation using PCG solver

The critical part of the FE computation of such a large model is the solver. For the current micro-FE analyses of voxel models of trabecular bone is one level element-by-element preconditioned conjugate gradient (EBE-PCG) Hughes et al (1987) considered as the most frequently used solver. The solver takes advantage of the identical size of every element in the voxel model (every element has exactly the same stiffness matrix) and it is very memory efficient (it does not compute the global stiffness matrix) since it requires only a matrix-vector product. However, due to its slow convergence and poor scalability, this solver is efficient only for problems of moderate size (under 1 million elements) and can be successfully used for the solution of small-volume samples of trabecular bone. For large models of whole bones or for nonlinear material models (plasticity) this solver is inefficient. An example of this inefficiency is given in van Rietbergen et al (2003) where linear elastic analysis of a micro-FE model of the proximal femur with 96 million elements using the EBE-PCG solver with a convergence tolerance of 10^{-3} took 25,000 CPU hours (almost 7 weeks of wall-clock time) on 30 processors of an SGI-Origin2000 computer with 250MHz-R10000 processors using 17 GB of memory.

For our computations, PCG solver with 1.10^{-8} tolerance was chosen for all considered FE models [Bangerth et al (2007), Bangerth et al (2011)]. Prior the computations with the largest system (rat vertebra, $\sim15.10^6$ unknowns) the convergence and speedup was tested using smaller FE models. These models were obtained by cutting the trabecular bone microstructure to smaller connected volumes with variable number of degrees of freedom (DOF). The cutting resulted in three FE models: i) small ($\sim$10,000 DOFs), ii) middle ($\sim$400,000 DOFs) and iii) large($\sim$3,000,000 DOFs).

On the SGI Altix 4700 the PCG solver scaled nicely up to 32 CPUs (more CPUs were not tested due to the workload of the computer by other users). Of course, the smallest FE model was not tested for more than 2 CPUs, since the solver took less then 3 seconds to converge on 1 CPU on the SGI Altix and less than 2 seconds on 1 core of Intel Xeon X5560. However, when number of unknows was larger than 100,000 the problems scaled very nicely on the SGI Altix system. As one can see from Tab. 1 the Intel Xeon X5660 system scaled nicely only up to 8 processor cores. Time needed to finish the large model using all 16 CPU cores was even larger when only 8 CPU cores were used. This might be caused by the fact, that the system was not fully-dedicated for the only task and there was no scheduling system available.

Tab. 1: Solver time and speedup for the middle-size model (400,000 DOFs) using PCG solver on SGI Altix 4700 architecture (Intel IA-64 Madison)

number of CPUs	solver time [s]	number of iterations	speedup [-]
1	663	205	1
2	404	250	1.6
4	250	265	2.7
8	106	275	6.3
16	59	286	11.2
32	30	303	22.1

Tab. 2: Solver time and speedup for large model (3,000,000 DOFs) using PCG solver on 16-core shared-memory Intel Xeon X5560 system

number of CPUs	solver time [s]	number of iterations	speedup [-]
1	1194	479	1
2	653	496	1.8
4	366	514	3.3
8	208	525	5.7
16	211	545	5.7

For the large problem, the SGI Altix was tested only from 8 CPUs up, since the NUMAlink architecture does not allow to allocate more than 2 GB RAM per processor and the memory needed for this problem was larger then the limit for smaller number of CPUs when used in parallel.

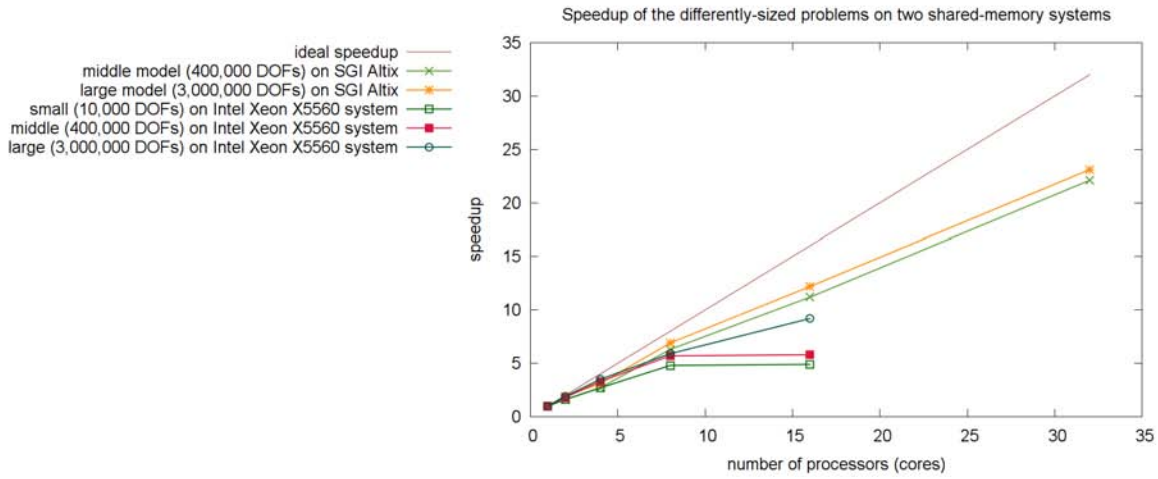

Fig. 3: Speedup of the PCG solver for differently-sized problems on the two architectures

3. Conclusions

In the paper, solution strategy for large-scale FE models originating from micro-CT data of trabecular microstructure of whole bones was presented. These micro-FE models are intended for validation of computationally less-demanding numerical models, but can be successfully used for numerical studies of implant-bone interaction, for studies of different approaches to vertebroplasty or in animal models for verification and comparison of drug treatments.

Results from the FE simulations were written in large ASCII files in both VTK (visualization toolkit, [Schroeder et al (2003)]) and GMV (general mesh viewer, [Ortega (2005)]) formats. The advantage of using VTK format lies in the easy postprocessing with Paraview [Henderson (2007)] which takes advantage of the multicore system (ParaView can be configured for visualization clusters using MPI parallel server on the same machine that is running the GUI).

From the inverse calculation of the orthotropic properties of micro-FE model of trabecular bone sample E_X=1.06 GPa, E_Y=1.97 GPa and E_Z=1.86 GPa were determined with agreement to previously published results, see Jirousek and Zlamal (2011).

Since the memory requirements for the PCG solver are slightly over 1 GB per million DOFs, one can easily compute the maximal number of unknowns solvable on a shared memory system. In our computations, a specialized program for partitioning graphs and FE meshes which produces fill reducing orderings for sparse matrices, METIS [Karypis and Kumar (1999)] was used. One limitation exists for the SGI Altix systems - the memory available for one processor is limited (in our configuration, each processor is eqquipped with 2 GB RAM) and therefore the user must decide how to partition the problem not to exceed the memory available for the single processor. On the other hand, the extensibility of the Altix 4700 is remarkable – the system can contain up to 2048 dual-core Itanium 2 processors (connected by the NUMAlink 4 interconnect) equipped by up to 128 TB of memory.

As a conclusion, it can be stated, that for very-large problems with more than 10 million unknowns the EBE-PCG solver (despite its low memory requirements) is inconvenient due to its slow convergence. In this case, more powerful and more scalable strategy should be employed, such as the Algebraic Multigrid (AMG) solvers, such in Eswaran et al (2007).

Acknowledgments

The research has been supported by RVO: 68378297 and by the Czech Science Foundation (grant No. P105/10/2305).

References

J.-Y. Rho, T. Y. Tsui, G. M. Pharr. (1997), Elastic properties of human cortical and trabecular lamellar bone measured by nanoindentation. *Biomaterials*, Vol 18, No. 20, pp. 1325–1330.

P. K. Zysset, X. E. Guo, C. E. Hoffler, K. E. Moore, S. A. Goldstein. (1999), Elastic modulus and hardness of cortical and trabecular bone lamellae measured by nanoindentation in the human femur. *Journal of Biomechanics*, Vol 32, No. 10, pp. 1005–1012.

O. Jirousek, J. Nemecek, D. Kytyr, J. Kunecky, P. Zlamal, T. Doktor. (2011), Nanoindentation of trabecular bone-comparison with uniaxial testing of single trabecula. *Chemicke Listy*, Vol 105, No. 17, pp. s668–s671.

B. Van Rietbergen, R. Muller, D. Ulrich, P. Ruegsegger, R. Huiskes. (1999), Tissue stresses and strain in trabeculae of a canine proximal femur can be quantified from computer reconstructions. *Journal of Biomechanics*, Vol 32, No 2, pp. 165–173.

G. L. Niebur, M. J. Feldstein, J. C. Yuen, T. J. Chen, T. M. Keaveny. (2000), High-resolution finite element models with tissue strength asymmetry accurately predict failure of trabecular bone. *Journal of Biomechanics*, Vol 33, No 12, pp. 1575–1583.

R. Jungmann, M. E. Szabo, G. Schitter, R. Yue-Sing Tang, D. Vashishth, P. K. Hansma, P.J. Thurner. (2011), Local strain and damage mapping in single trabeculae during three-point bending tests. *Journal of the Mechanical Behavior of Biomedical Materials*, Vol 4, No. 4, pp. 523–534.

T. Doktor, O. Jirousek, D. Kytyr, P. Zlamal, I. Jandejsek. (2011), Real-time X-ray microradiographic imaging and image correlation for local strain mapping in single trabecula under mechanical load. *Journal of Instrumentation*, Vol 6, No. 11 , Art.No. C11007.

S. Lorenzetti, R. Carretta, R. Muller, E. Stussi. (2011), A new device and method for measuring the elastic modulus of single trabeculae. *Medical Engineering and Physics*, Vol 33, No. 8, pp. 993–1000.

R. Muller, P. Ruegsegger. (1995) Three-dimensional finite element modelling of non-invasively assessed trabecular bone structures. *Medical Engineering and Physics*, Vol 17, No. 2, pp. 126–133.

R. Natarajan. (1991), Finite element applications on a shared-memory multiprocessor: Algorithms and experimental results. *Journal of Computational Physics*, Vol 94, No. 2, pp. 352–381.

B. C. Hodgson, P. K. Jimack. (1997), A domain decomposition preconditioner for a parallel finite element solver on distributed unstructured grids. *Parallel Computing*, Vol 23, No. 8, pp. 1157–1181.

Z. Johan, K. K. Mathur, S. L. Johnsson, T. J. R. Hughes. (1994), Scalability of finite element applications on distributed-memory parallel computers. it Computer Methods in Applied Mechanics and Engineering, Vol 119, No. 12, pp. 61–72.

J. A. MacNeil, S. K. Boyd. (2008) Bone strength at the distal radius can be estimated from high-resolution peripheral quantitative computed tomography and the finite element method. *Bone*, Vol 42, No. 6, pp. 1203-1213.

S. K. Eswaran, H. H. Bayraktar, M. F. Adams, A. Gupta, P. F. Hoffmann, D. C. Lee, P. Papadopoulos, T. M. Keaveny. (2007), The micro-mechanics of cortical shell removal in the human vertebral body. Computer Methods in Applied Mechanics and Engineering, Vol 196, No. 3132, pp. 3025-3032.

F. Taddei, A. Pancanti, M. Viceconti. (2004), An improved method for the automatic mapping of computed tomography numbers onto finite element models. *Medical Engineering and Physics*, Vol 26, No. 1, pp. 61–69.

D. H Pahr and P. K Zysset. (2009), A comparison of enhanced continuum FE with micro FE models of human vertebral bodies. *Journal of Biomechanics*, Vol 42, No. 4, pp 455–62.

W. E. Lorensen, H. E. Cline. (1987), Marching Cubes: A high resolution 3D surface construction algorithm. *Computer Graphics*, Vol. 21, No. 4, pp. 163–169.

Y. Chevalier, D. Pahr, H. Allmer, M. Charlebois, P. Zysset. (2007), Validation of a voxel-based FE method for prediction of the uniaxial apparent modulus of human trabecular bone using macroscopic mechanical tests and nanoindentation. *Journal of Biomechanics*, Vol 40, No. 15, pp. 3333–3340.

D. Vavrik, J. Jakubek. (2009), Radiogram enhancement and linearization using the beam hardening correction method. *Nuclear Instruments and Methods in Physics Research Section A*, Vol 607, No 1, pp 212–214.

N. Otsu. (1979). A Threshold Selection Method from Gray-Level Histograms. *IEEE Transactions on Systems, Man, and Cybernetics*, Vol. 9, No. 1, pp. 62–66.

T. J. R. Hughes, R. M. Ferencz, and J. O. Hallquist. (1987), Large-scale vectorized implicit calculation in solid mechanics on a Cray X-MP/48 utilizing EBE preconditioned conjugate gradients, *Computer Methods in Applied Mechanics and Engineering*, Vol 61, pp 215-248.

B. van Rietbergen, R. Huiskes, F. Eckstein, and P. Ruegsegger. (2003), Trabecular bone tissue strains in the healthy and osteoporotic human femur. *Journal of Bone and Mineral Research*, Vol 18, No. 10, pp 1781–1788.

G. Karypis and V. Kumar. (1999), A Fast and Highly Quality Multilevel Scheme for Partitioning Irregular Graphs. *SIAM Journal on Scientific Computing*, Vol. 20, No. 1, pp. 359392.

W. Bangerth and R. Hartmann and G. Kanschat. (2007) deal.II – a General Purpose Object Oriented Finite Element Library. *ACM Transactions on Mathematical Software*, Vol 33, No. 4, pp. 24/1–24/27.

W. Bangerth, C. Burstedde, T. Heister, M. Kronbichler. (2011), Algorithms and Data Structures for Massively Parallel Generic Finite Element Codes. *ACM Transactions on Mathematical Software*, Vol 38, No. 2, pp. 14:1–14:28.

W. Schroeder et al. (2003) The Visualization Toolkit. 3rd Edition. Kitware Inc.

F. A. Ortega. GMV 3.8. General Mesh Viewer Users Manual. (2005), Los Alamos National Laboratory, http://www-xdiv.lanl.gov/XCM/gmv

A. Henderson. (2007), ParaView Guide, A Parallel Visualization Application. *Kitware Inc.*

O. Jirousek, and P. Zlamal. (2011) Microstructural models of trabecular bone -comparison of CT-based FE models. *17^{th} International Conference Engineering Mechanics 2011*, Vol 1, No. 1, pp. 247–250.